Journal of Organometallic Chemistry 694 (2009) 1027–1035

Contents lists available at ScienceDirect

Journal of Organometallic Chemistry

journal homepage: www.elsevier.com/locate/jorganchem

Synthesis and structure of mono- and dinuclear cyclopentadienyl–indenyl complexes of iron(II) and further reactions to mixed tri- and tetranuclear iron–cobalt complexes

Shengli Guo, Ildiko Balog, Ralf Hauptmann, Mathias Nowotny, Jörg J. Schneider *

Eduard-Zintl-Institut für Anorganische und Physikalische Chemie, Technische Universität Darmstadt, Petersenstraße 18, 64287 Darmstadt, Germany

ARTICLE INFO

Article history:
Received 9 September 2008
Received in revised form 17 October 2008
Accepted 7 November 2008
Available online 20 November 2008

Dedicated to Prof. Christoph Elschenbroich on the occasion of his 70th birthday.

Keywords:
Metallocenes
Indenyl ligands
Cobalt
Iron

ABSTRACT

The reaction of a mixture of sodium cyclopentadienide and the monolithium salt or dilithium salt of 2,2-bis(indenyl)propane with $FeCl_2$ leads to the mononuclear complex $[(\eta^5\text{-}C_5H_5)Fe(\eta^5\text{-ind-}C(CH_3)_2\text{-ind})]$ (ind = 1-indenyl) (**1**) and the dinuclear complex $[\{(\eta^5\text{-}C_5H_5)Fe(\eta^5\text{-ind})\}_2C(CH_3)_2]$ (**2**), respectively. $[(\eta^5\text{-}Me_5C_5)Fe(tmeda)Cl]$ reacts with dilithium 1,1′-biindenyl under formation of $[\{(\eta^5\text{-}Me_5C_5)Fe\}_2(\mu\text{-}\eta^5\text{:}\eta^5\text{-}1,1'\text{-biind})]$ (**4**). Due to the annelated arene rings of the η^5-indenyl ligands, **2** and **4** may act as 4-electron donor ligands, as exemplified by the reaction with the triple-decker complex $[\{(\eta^5\text{-}Me_5C_5)Co\}_2(\mu\text{-}\eta^6\text{:}\eta^6\text{-toluene})]$, which afforded the tetranuclear dimer of triple-decker complexes $[\{(\eta^5\text{-}C_5H_5)Fe(\eta^5\text{-}Me_5C_5)Co(\mu\text{-}\eta^5\text{:}\eta^4\text{-1-ind})\}_2C(CH_3)_2]$ (**3**) and the trinuclear complex $[\{(\eta^5\text{-}Me_5C_5)Fe\}_2(\eta^5\text{-}Me_5C_5)Co(\mu_3\text{-}\eta^5\text{:}\eta^4\text{:}\eta^5\text{-}1,1'\text{-biind})]\cdot Et_2O$ (**5** · Et_2O) by replacement of the central toluene deck, respectively. The $[(\eta^5\text{-}Me_5C_5)Co]$ fragments of **3** and **5** are bonded via the six-membered rings of the indenyl ligands in a η^4-fashion. Caused by the coordination to the Co atoms the six-membered rings lose their planarity and adopt a butterfly structure. The coordination geometry of the Fe atoms is similar in all five complexes. Each Fe atom is coordinated by the C atoms of one of the five-membered rings of the indenyl ligands in a slightly distorted η^5 manner ($\eta^3 + \eta^2$-coordination) and by a cyclopentadienyl ligand in a regular η^5-fashion. The structures of **3** and **5** represent the first examples of slipped triple-decker complexes which comprise indenyl ligands in a $\mu\text{-}\eta^5\text{:}\eta^4$ coordination mode.

1. Introduction

Indenyl complexes of the composition $[(\eta^5\text{-ind})ML_n]$ have been intensely studied during the past decades, since they display enhanced reactivity by comparison to their cyclopentadienyl analogues in both $S_N1$and S_N2 substitution reactions [1], and also by intermolecular hydroacylation reactions [2], cyclotrimerization of alkenes to benzenes [3,4] and cyclotrimerization of alkenes and nitriles to pyridines [5]. The reason for this enhanced reactivity, which is commonly referred to as indenyl effect, is generally attributed to a re-aromatization of the fused arene ring in the transition state. The chemistry of indenyl metal complexes has been summarized in several recent reviews [6–8]. The presence of two fused π-systems in the indenyl system enables this bicyclic arene to act as a bridging ligand in homo- and heterobinuclear complexes $[L_nM(\mu\text{-}\eta\text{:}\eta\text{-ind})M'L'_n]$. However, examples for such a bridging coordination mode are still relatively rare [9–14], and especially in the area of multidecker sandwich complexes the number of structurally characterized examples is limited to few examples in which indenyl acts as a central $\mu\text{-}\eta^5\text{:}\eta^6$-bridge between $[(\eta^5\text{-}C_5(R)_5)Ru]$ (R = H, CH_3) and $[(\eta^4\text{-}C_4(CH_3)_4)Co]$ fragments [15,16].

Triple-decker complexes of the type $[\{(\eta^5\text{-}Me_5C_5)Co\}_2(\mu\text{-arene})]$ (arene = benzene, toluene, iso-propylbenzene, o-, m-, p-xylene) are highly reactive synthons for the transfer of $(\eta^5\text{-}Me_5C_5)Co$ fragments, since the central arene ligand is bonded very weakly. They are accessible in a reductive ligand degradation from $[(\eta^5\text{-}Me_5C_5)Co(O,O'\text{-acac})]$ [17] by potassium metal in various arenes [18]. It is possible to substitute the arene middle deck under mild conditions by various other arenes [18–20]. Therefore, it should also be possible to use arene–metal complexes with non-coordinated ring systems as ligands to substitute the toluene molecule and thereby to prepare compounds of higher nuclearity and mixed metal complexes.

Here, we present the synthesis and crystal structure of new mixed iron indenyl–cyclopentadienyl complexes and the products of their reaction with the labile triple-decker complex $[\{(\eta^5\text{-}Me_5C_5)Co\}_2(\mu\text{-}\eta^6\text{:}\eta^6\text{-toluene})]$.

2. Results and discussion

The straightforward approach of reacting a 1:1 mixture of sodium cyclopentadienide and the monolithium salt of 2,2-bis

* Corresponding author. Tel.: +49 6151 163224; fax: +49 6151 163470.
E-mail address: joerg.schneider@ac.chemie.tu-darmstadt.de (J.J. Schneider).

0022-328X/$ - see front matter © 2008 Elsevier B.V. All rights reserved.
doi:10.1016/j.jorganchem.2008.11.024

(1-indenyl)propane with 1 equiv. of $FeCl_2$ allows the isolation of the mononuclear complex [(η^5-C_5H_5)Fe(η^5-ind-C(CH_3)$_2$-ind)] (**1**) after chromatographic workup. An analogous reaction with a 2:1 mixture of sodium cyclopentadienide and the dilithium salt of 2,2-bis(1-indenyl)propane with 2 equiv. of $FeCl_2$ results in the formation of the dinuclear complex [{(η^5-C_5H_5)Fe(η^5-1-ind-)}$_2$-C(CH_3)$_2$] (**2**) as a mixture of racemic and meso isomers. A randomly chosen, well-shaped crystal from the mixture of isomers prove to consist of *meso*-**2** in a crystal structure analysis. The tetranuclear complex [{(η^5-C_5H_5)Fe(η^5-Me_5C_5)Co(μ-η^5:η^4-1-ind)}$_2$C(CH_3)$_2$] (*rac*-**3**) represents the only isolated product from the reaction between an isomer mixture of **2** and the triple-decker complex [{(η^5-Me_5C_5)Co}$_2$(μ-η^6:η^6-toluene)] (see Scheme 1).

[(η^5-Me_5C_5)Fe(tmeda)Cl] reacts with dilithium 1,1′-biindenyl under formation of [{(η^5-Me_5C_5)Fe}$_2$(μ-η^5:η^5-1,1′-biind)] (**4**) as a mixture of isomers, which due to steric reasons predominantly consists of the *meso*-form. Pure *meso*-**4** may be isolated by fractional crystallization. The reaction of *meso*-**4** with [{(η^5-Me_5C_5)Co}$_2$-(μ-η^6:η^6-toluene)] affords the trinuclear complex [{(η^5-Me_5C_5)-Fe}$_2$(η^5-Me_5C_5)Co(μ_3-η^5:η^4:η^5-1,1′-biind)] · Et_2O (**5** · Et_2O) (see Scheme 2).

2.1. Molecular structure of *1*, *meso*-*2* and *rac*-*3*

The coordination geometries adopted by the Fe atoms in the complexes **1**, *meso*-**2** and *rac*-**3** are closely related. Each Fe atom is coordinated by the C atoms of one of the five-membered rings of the 2,2-bis(1-indenyl)propane ligand and by a cyclopentadienyl ligand in a η^5-fashion (see Figs. 1–3).

The Fe–C bond lengths to the cyclopentadienyl ligands are comparable and range from 1.992(10) to 2.069(6) Å. The averages are 2.007 Å in **1**, 2.044 and 2.046 Å in *meso*-**2**, and 2.050 and 2.053 Å in *rac*-**3**. Moreover, the Fe–C bond distances to the indenyl ligands are also similar in all three compounds and range from 2.025(11) to 2.095(6) Å. The averages of these Fe–C bond lengths are 2.058 Å in **1** and *meso*-**2**, and 2.062 and 2.057 Å in *rac*-**3**. All these Fe–C distances are in good agreement with the respective values reported for (η^5-4,7-dimethylindenyl)(η^5-pentamethylcyclopentadienyl)iron(II) [21] and bis(η^5-cyclopentadienyl)[1,1′-tetramethyldisiloxy-2,2′-bis(η^5-indenyl)]diiron(II) [22] and also with those values found in substituted bis(η^5-indenyl)iron(II) complexes [23]. The relatively large range of the Fe–C bond distances indicates that the η^5-coordination towards the indenyl ligand is not perfect, but displays some extent of ene-allyl distortion and is hence better described as a $\eta^3 + \eta^2$ mode. A similar distorted η^5-coordination has also been observed in virtually all structurally characterized indenyl complexes. This allyl-ene distortion is generally explained on the basis of the different contributions of the five C atoms in the coordinating ring to the π-orbitals of indenyl which are relevant for the bonding [24]. The C–C bond distances within the coordinating indenyl ring in **1** are in the expected range (1.369(11) to 1.445(11) Å) for an aromatic system. In the non-coordinating indenyl ring the C=C bond distances are in a similar range (1.353(13) to 1.431(11) Å), whereas the three C–C distances of the single bonds are in the range from 1.484(12) to 1.520(12) Å. In *meso*-**2** the C–C distances in the two coordinating indenyl rings range from 1.352(10) to 1.451(9) Å, and are comparable to the respective values in **1**.

The tetranuclear dimer of slipped triple-decker complexes *rac*-**3** results from the reaction between a mixture of isomers of **2** and the triple-decker complex [{(η^5-Me_5C_5)Co}$_2$(μ-η^6:η^6-toluene)]. In this reaction both of the annelated arene rings in **2** act as four-electron donor ligands and replace the bridging toluene ligand in [{(η^5-Me_5C_5)Co}$_2$(μ-η^6:η^6-toluene)]. The [(η^5-Me_5C_5)Co] fragments are bonded to the non-junction carbon atoms of the fused six-membered rings of the indenyl ligands in a η^4-fashion, while the non-bonding distances between the Co atoms and the junction carbon atoms span the range from 2.789(7) to 2.883(6) Å. To the best of our knowledge, complex *rac*-**3** represents the first structurally characterized example of a slipped triple-decker complex with a central indenyl deck in a μ-η^5:η^4 coordination mode. A similar η^4-coordination of the [(η^5-Me_5C_5)Co] fragment towards an arene is also observed in the crystal structure of the triple-decker precursor and other compounds of the composition [{(η^5-Me_5C_5)Co}$_2$(μ-arene)] (arene = benzene, toluene, iso-propylbenzene, o-, m-, p-xylene), though due to the a μ-η^4:η^4 bonding mode the arene bridge in these complexes is planar [18,19]. As expected for a η^4-coordinated diene system, the Co–C bond distances to the central carbon atoms C6, C7 and C18, C19, respectively, range from 1.952(7) to 1.975(6) Å and are therefore, significantly shorter than those distances between the Co atoms and the terminal carbon atoms of the diene system C5, C8 and C17, C20, respectively, which range

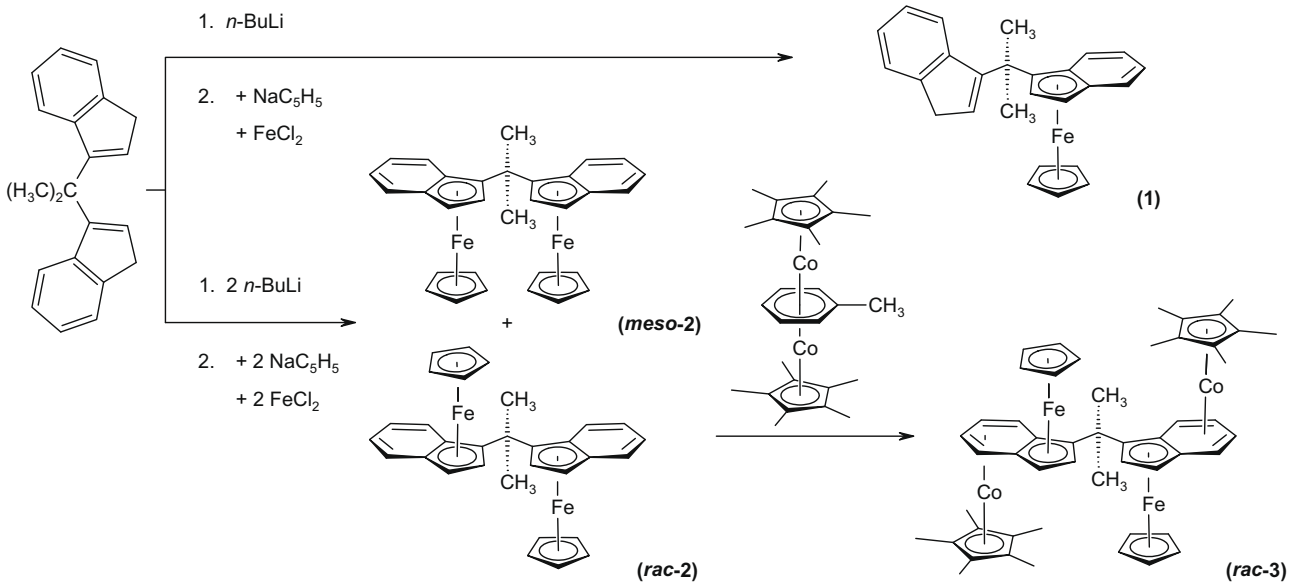

Scheme 1. Synthesis of complexes **1**, **2**, and **3**.

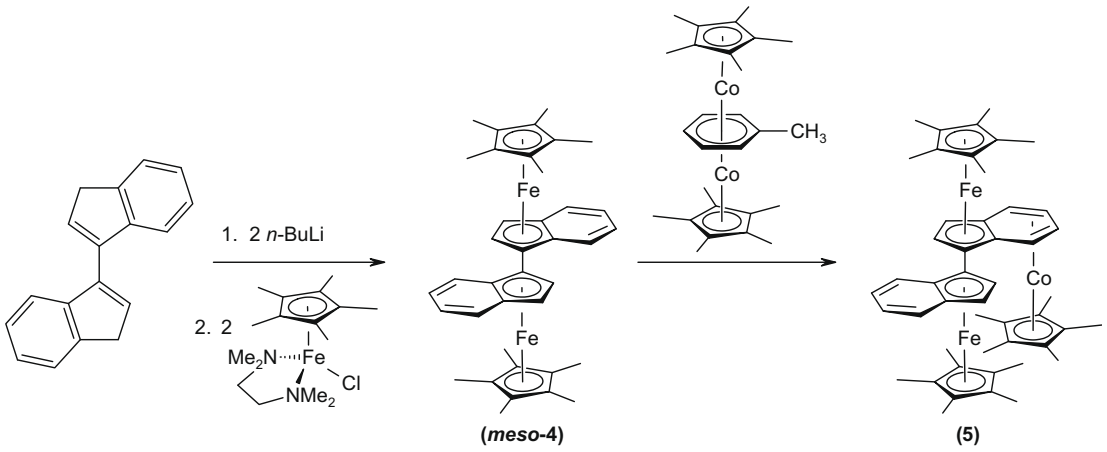

Scheme 2. Synthesis of the complexes **4** and **5**.

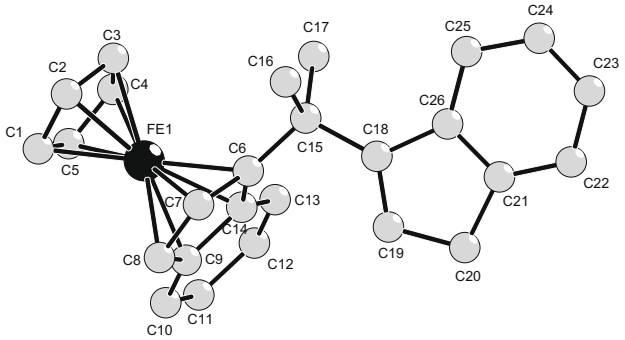

Fig. 1. Molecular structure of **1** (H atoms have been omitted for clarity). Selected bond distances [Å]: Fe1–C1 1.992(10), Fe1–C2 2.029(13), Fe1–C3 2.014(13), Fe1–C4 1.995(13), Fe1–C5 2.006(13), Fe1–C6 2.062(9); Fe1–C7 2.044(9), Fe1–C8 2.025(11), Fe1–C9 2.065(9), Fe1–C14 2.095(8).

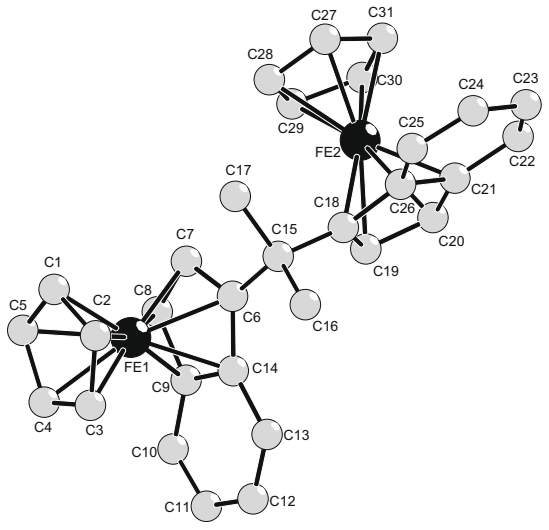

Fig. 2. Molecular structure of *meso*-**2** (H atoms have been omitted for clarity). Selected bond distances [Å]: Fe1–C1 2.051(7), Fe1–C2 2.055(7), Fe1–C3 2.042(6), Fe1–C4 2.044(7), Fe1–C5 2.030(6), Fe1–C6 2.059(6), Fe1–C7 2.044(6), Fe1–C8 2.039(7), Fe1–C9 2.072(7), Fe1–C14 2.076(6), Fe2–C18 2.069(6), Fe2–C19 2.041(6), Fe2–C20 2.027(6), Fe2–C21 2.060(6), Fe2–C26 2.095(6), Fe2–C27 2.039(7), Fe2–C28 2.056(7), Fe2–C29 2.047(6), Fe2–C30 2.053(7), Fe2–C31 2.033(7).

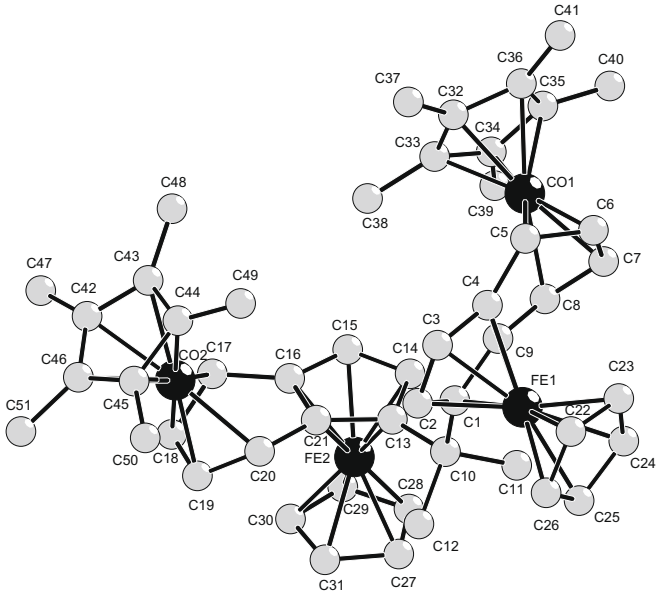

Fig. 3. Molecular structure of *rac*-**3** (H atoms have been omitted for clarity). Selected bond distances [Å]: Fe1–C1 2.065(6), Fe1–C2 2.026(7), Fe1–C3 2.048(6), Fe1–C4 2.079(6), Fe1–C9 2.094(6), Fe1–C22 2.053(7), Fe1–C23 2.039(8), Fe1–C24 2.037(8), Fe1–C25 2.069(6), Fe1–C26 2.052(7), Fe2–C13 2.058(6), Fe2–C14 2.029(6), Fe2-C15 2.042(6), Fe2–C16 2.079(5), Fe2–C21 2.079(5), Fe2–C27 2.066(6), Fe2–C28 2.064(6), Fe2–C29 2.054(6), Fe2–C30 2.042(7), Fe2–C31 2.041(6), Co1–C5 2.065(6), Co1–C6 1.966(6), Co1–C7 1.975(6), Co1–C8 2.093(6), Co1–C32 2.040(6), Co1–C33 2.036(6), Co1–C34 2.039(6), Co1–C35 2.107(6), Co1–C36 2.085(6), Co2–C17 2.071(6), Co2–C18 1.952(7), Co2–C19 1.956(6), Co2–C20 2.096(6), Co2–C42 2.073(7), Co2–C43 2.076(6), Co2–C44 2.063(7), Co2–C45 2.052(7), Co2–C46 2.076(7).

from 2.065(6) to 2.096(6) Å. Further support for the η^4-coordination mode of the indenyl systems to the [(η^5-Me_5C_5)Co] fragments derives from the fact, that both six-membered rings of the 2,2-bis(indenyl)propane ligand lose their planarity and adopt a butterfly structure. The angles between the two planes are 34.0(3)° in the case of (C4, C5, C8, C9):(C5, C6, C7, C8) and 37.0(3)° for (C16, C17, C20, C21):(C17, C18, C19, C20). The C–C bond lengths between the junction carbon atoms which are coordinated to the Fe atoms and the terminal carbon atoms of the diene system which are bound to the Co atoms (C4–C5, C8–C9, C16–C17, C20–C21) range from 1.468(8) to 1.481(8) Å and are therefore significantly longer than the other C–C bond distances in the indenyl system, which range from 1.409(9) to 1.449(8) Å. The average distance between the junction carbon atoms of the indenyl bridges (C4–C9, C16–C21) of 1.423(8) Å compares well with the average of all C–C distances

of the five-membered indenyl rings, which amounts to 1.429(9) Å. Hence, a significant elongation of the respective bond, as it had been reported for slipped triple-decker complexes bearing an indenyl bridge in a μ-η^5:η^6 bonding mode [15,16], is not observed in the structure of *rac*-**3**. This fact may be ascribed to the different bonding situation of the junction carbon atoms in *rac*-**3**, which do not bridge two metal centers, but are coordinated exclusively to the respective Fe atoms. The Co–C bond lengths to the pentamethylcyclopentadienyl ligands in *rac*-**3** range from 2.036(6) to 2.107(6) Å with averages of 2.061(6) Å for Co1 and 2.068(6) Å for Co2. The C–C bonds in the pentamethylcyclopentadienyl ligands are all in a normal range.

2.2. Molecular structure of meso-4 and 5

The coordination of the Fe atoms in *meso*-**4** and **5** resembles that of the complexes **1**, *meso*-**2** and *rac*-**3** (see Figs. 4 and 5). The Fe atoms are coordinated by the C atoms of one of the five-membered rings of the biindenyl ligand ($\eta^3 + \eta^2$-fashion) and by a pentamethylcyclopentadienyl ligand (η^5-fashion).

As in **1**, *meso*-**2**, and *rac*-**3** the range of the Fe–C bonds to the indenyl ligand is relatively large (2.012(4) to 2.118(4) Å), thereby indicating a distorted $\eta^3 + \eta^2$-coordination. In contrast, all Fe–C bond distances to the pentamethylcyclopentadienyl ligands are comparable and range from 2.043(3) to 2.080(5) Å. The averages are 2.055 Å in *meso*-**4**, and 2.063 and 2.054 Å in **5**. These values are similar to those in **1**, *meso*-**2** and *rac*-**3** and are also in good agreement with previously reported data [21,22].

Similar to the structure of *rac*-**3**, the [(η^5-Me_5C_5)Co] fragment in **5** coordinates to the annelated arene ring of one of the indenyl units in a η^4-fashion. The bond lengths between the Co atom and the carbon atoms of the coordinated diene system of the indenyl ligand in **5** split, as observed in *rac*-**3**, into two sets. The average bond length towards the central carbon atoms of the diene system C16 and C17 amounts to 1.967(5) Å, whereas the bond distance towards the terminal carbon atoms C15 and C18 averages to 2.122(4) Å. In contrast, the average distance between Co1 and the junction carbon atoms C14 and C19 amounts to 2.883(4) Å. Moreover, the six-membered ring of the bridging indenyl ligand is folded along the vector C15–C18. The angle between the two planes (C14, C15, C18, C19) and (C15, C16, C17, C18) amounts to 35.2(2)° and is in good agreement with the respective value in **3**. Contrarily, the analogous angle in the non-coordinating six-membered ring of **5** is 0.9(7)°, in accordance with the expected planarity. The C–C bond lengths within the bridging μ-η^5:η^4-indenyl ligand show the same features as those observed in **3**. The C–C distances between the junction carbon atoms which bind to Fe1 and the adjacent C atoms which are coordinated to Co1 (C14–C15 1.470(6) and C18–C19 1.482(6) Å) are significantly longer than the other C–C bond distances which range from 1.427(6) to 1.449(5) Å. The distance between the junction carbon atoms C14 and C19 of the μ-η^5:η^4-indenyl ligand in **5** amounts to 1.434(6) Å, which is not noticeably longer than the average C–C distance within the five-membered ring of 1.439(6) Å, hence in accordance with the structure of **3** a lengthening of this bond can be ruled out. In the non-bridging indenyl ring which is only coordinated to Fe2 in a η^5-fashion the C–C bond lengths span the range from 1.361(7) to 1.465(6) Å.

Complex **5** crystallizes with one molecule of ether as crystal solvent. This ether molecule shows no interaction with the complex molecule.

Common parameters for the comparison of the extent of slip-fold distortion in the solid-state structures of bis(η^5-indenyl)metal complexes are the slip parameter Δ, the hinge angle HA, the fold angle FA and the rotation angle RA [25]. The slip parameter Δ is defined as the difference between the average bond length of the metal atom to the junction carbon atoms, C3a, C7a and the average bond length of the metal to the adjacent carbon atoms of the five-membered ring, C1, C3: Δ = avg. d(M-C3a, C7a) – avg. d(M-C1, C3). In bis(indenyl) complexes HA is defined as the angle

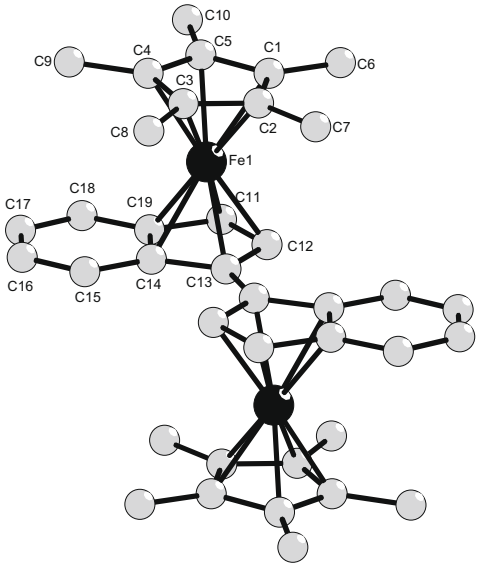

Fig. 4. Molecular structure of *meso*-**4** (H atoms have been omitted for clarity). Selected bond distances [Å]: Fe1–C1 2.043(3), Fe1–C2 2.048(3), Fe1–C3 2.057(3), Fe1–C4 2.068(3), Fe1–C5 2.058(3), Fe1–C11 2.074(3), Fe1–C12 2.054(3), Fe1–C13 2.083(2), Fe1–C14 2.102(2), Fe1–C19 2.108(3).

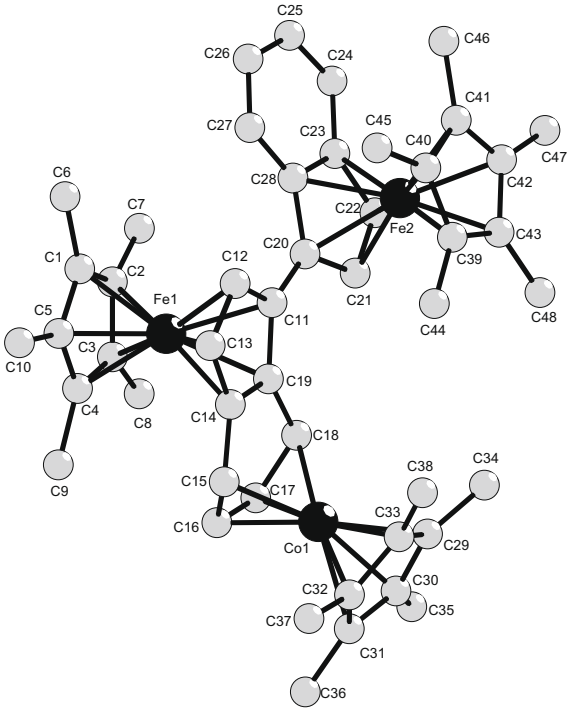

Fig. 5. Molecular structure of **5** (H atoms have been omitted for clarity). Selected bond distances [Å]: Fe1–C1 2.068(5), Fe1–C2 2.080(5), Fe1–C3 2.052(5), Fe1–C4 2.063(5), Fe1–C5 2.054(5), Fe1–C11 2.091(4), Fe1–C12 2.024(4), Fe1–C13 2.064(4), Fe1–C14 2.097(4), Fe1–C19 2.118(4), Fe2–C20 2.095(4), Fe2–C21 2.052(4), Fe2–C22 2.059(4), Fe2–C23 2.103(4), Fe2–C28 2.097(4), Fe2–C39 2.055(4), Fe2–C40 2.056(4), Fe2–C41 2.052(4), Fe2–C42 2.057(5), Fe2–C43 2.048(5), Co1–C15 2.104(4), Co1–C16 1.962(5), Co1–C17 1.973(5), Co1–C18 2.140(4), Co1–C29 2.084(4), Co1–C30 2.101(4), Co1–C31 2.107(4), Co1–C32 2.062(4), Co1–C33 2.079(5).

between planes (C1, C2, C3) and (C1, C3, C3a, C7a). For defining the HA of the cyclopentadienyl ligand in the mixed indenyl-cyclopentadienyl complexes presented here we used the angle between the plane (C1b, C2b, C3b) and (C1b, C3b, C4b, C5b). For indenyl ligands FA is generally defined as the angle between the planes (C1, C2, C3) and (C3a, C4, C5, C6, C7, C7a). In bis(indenyl) complexes RA is the angle between the planes formed by C2, the metal and the midpoint of the C3a–C7a bond in one case, and C2′, the metal and the midpoint of the C3a′–C7a′ bond in the other case. For the mixed cyclopentadienyl–indenyl Fe complexes presented here we define RA as the angle between the planes (C2, Fe, midpoint C3a–C7a) and (C2b, Fe, midpoint C4b–C5b) (Scheme 3).

The values for Δ, HA, FA and RA are summarized in Table 1. Indenyl complexes that show values of HA and Δ less than 10° and 0.25 Å, respectively, are generally considered to be η^5. The respective values of HA and Δ of all complexes presented here lie well below these limits, thereby supporting the description of the coordination of the indenyl ligand to the Fe atoms as η^5 with only little extent of slip-fold distortion. A remarkable feature is the large value for FA displayed by **3** and **5**. These pronounced deviations are obviously caused by the loss of planarity of the six-membered rings due to the η^4-coordination to the Co atoms, which significantly affects the accuracy of definition of a best plane through the respective carbon atoms. In order to obtain a more reliable distortion parameter, we hence introduced a modified fold angle FA′ defined as the angle between the planes (C1, C2, C3) and (C3a, C4, C7, C7a). The values of FA′ shown by **3** and **5** lie well within the typical range of FA reported for η^5-indenyl complexes. The variety of values for RA displayed by the presented complexes should be caused predominantly by packing effects.

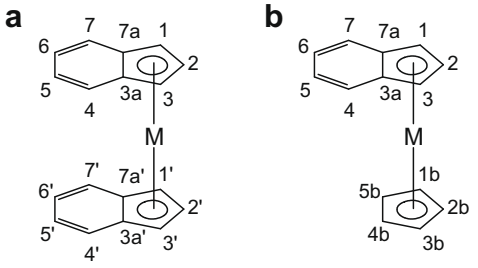

Scheme 3. Definition of the hinge angle HA, fold angle FA and rotation angle RA for bis(indenyl) complexes (a) and mixed cyclopentadienyl–indenyl complexes (b). (a) HA = (C1, C2, C3):(C1, C3, C3a, C7a); FA = (C1, C2, C3):(C3a, C4, C5, C6, C7, C7a); RA = (C2, M, mid. C3a-C7a):(C2′, M, mid. C3a′–C7a′). b) HA(ind) = (C1, C2, C3):(C1, C3, C3a, C7a); HA(cp) = (C1b, C2b, C3b):(C1b, C3b, C4b, C5b); FA(ind) = (C1, C2, C3):(C3a, C4, C5, C6, C7, C7a); FA′(ind) = (C1, C2, C3):(C3a, C4, C7, C7a); RA = (C2, Fe, mid. C3a–C7a) and (C2b, Fe, mid. C4b–C5b).

2.3. ^1H and ^{13}C spectroscopic properties of **1**, **2**, **3**, **4** and **5**

The coordination of the {(η^5-Me_5C_5)Co} fragment to the six-membered rings of the indenyl groups leads to a characteristic upfield shift for H4–H7 in **3** and **5** (numbering according to Scheme 3). These shifts are comparable to those found in other complexes with η^4-coordinated annelated arene ligands (Table 2).

An analogous upfield shift caused by the coordination of the {(η^5-Me_5C_5)Co} fragment was also observed for the signals of C4–C7 in the ^{13}C NMR spectra of **3** and **5**. The coordination shift $\Delta(^{13}C)$ in **3** with respect to **2** amounts to 76 ppm for C4 and C7 and 41 ppm for C5 and C6. The respective values for **5** in comparison with **4** are very similar (78 ppm for C4 and C7, and 39 ppm for C5 and C6).

The ^1H and ^{13}C shifts for the {(η^5-Me_5C_5)Co} fragments in **3** and **5** are comparable to those of [{(η^5-Me_5C_5)Co}$_2$(μ-η^6:η^6-toluene)] [18]. The location of the ^1H and ^{13}C signals of the {(η^5-C_5H_5)Fe} and {(η^5-C_5Me_5)Fe} fragments in the NMR spectra of all complexes presented here are in good agreement with the respective values reported for ferrocene [26,27] and decamethylferrocene [28].

2.4. Electrochemical properties of **1**, **2** and **4**

The cyclic voltammograms (CV) for **1**, **2** and **4** in DME/0.1M *n*-Bu_4NBF_4 are presented in Fig. 6, relevant data are collected in Table 3.

The CV traces display two clearly separated regions: Fe-centered reduction ($-3.0 < E < -2.0$ V) and Fe-centered oxidation ($0 < E < 0.5$ V). The binuclear complexes **2** and **4** display reversible, overlapping oxidations to the Fe^{III}–Fe^{II} and Fe^{III}–Fe^{III} mono- and dications. In addition, **2** shows reversible, overlapping reductions

Table 2
Comparison of the ^1H-chemical shift of the protons of η^4-coordinated annelated arene ligands.

	H4, H7	H5, H6
3 (This work)	2.21, 2.41	5.76, 5.92
5 (This work)	2.19, 2.49	6.10, 6.13
[{(η^5-Me_5C_5)Co}$_2$$\mu$-($\eta^5$:$\eta^4$-fluorenone)] [20]	1.79, 2.35	6.04, 6.15
[{(η^5-$EtMe_4C_5$)Co}$_2$$\mu$-($\eta^5$:$\eta^4$-fluorenone)] [20]	1.57, 2.39	6.08, 6.18
[(η^5-Me_5C_5)Co(η^4-anthracene)] [19]	2.52	5.68
[{(η^5-Me_5C_5)Co}$_2$$\mu$-($\eta^4$:$\eta^4$-anthracene)] [19]	2.08	5.93
[(η^5-Me_5C_5)Co(η^4-naphthalene)] [19]	1.98	5.70

Table 1
Comparison of the coordination of the Fe atoms by the parameters Δ, HA, FA and RA for **1**, **2**, **3**, **4** and **5**.

	M	Ligand	Δ (Å)	HA (°)	FA (°)	FA′ (°)	RA (°)
1	Fe1	cpi nd	[a]0.037(9)	0.10(87) (cp) 2.78(68) (ind)	[a]1.54(48)	[a]1.04(51)	6.00(47)
2	Fe1	cp	[a]0.025(7)	0.14(37) (cp)	[a]0.88(46)	[a]0.80(49)	9.66(21)
		ind		2.05(39) (ind)			
	Fe2	cp	[a]0.030(6)	1.04(51) (cp)	[a]3.11(44)	[a]2.68(42)	3.58(13)
		ind		3.05(46) (ind)			
3	Fe1	cp	[a]0.030(6)	1.35(54) (cp)	[a]12.45(38)	[a]4.02(45)	9.13(19)
		ind		0.90(39) (ind)			
	Fe2	cp	[a]0.029(6)	0.08(27) (cp)	[a]14.66(50)	[a]2.53(53)	6.95(24)
		ind		1.45(55) (ind)			
4	Fe1	cp	[a]0.027(3)	0.47(19) (cp)	[a]2.01(15)	[a]1.70(16)	25.73(9)
		ind		1.71(18) (ind)			
5	Fe1	cp	[a]0.030(4)	0.28(26) (cp)	[a]13.41(35)	[a]2.96(36)	5.09(13)
		ind		0.34(34) (ind)			
	Fe2	cp	[a]0.023(4)	0.63(32) (cp)	[a]1.98(26)	[a]1.69(24)	20.82(13)
		ind		1.36(31) (ind)			

[a] Not defined.

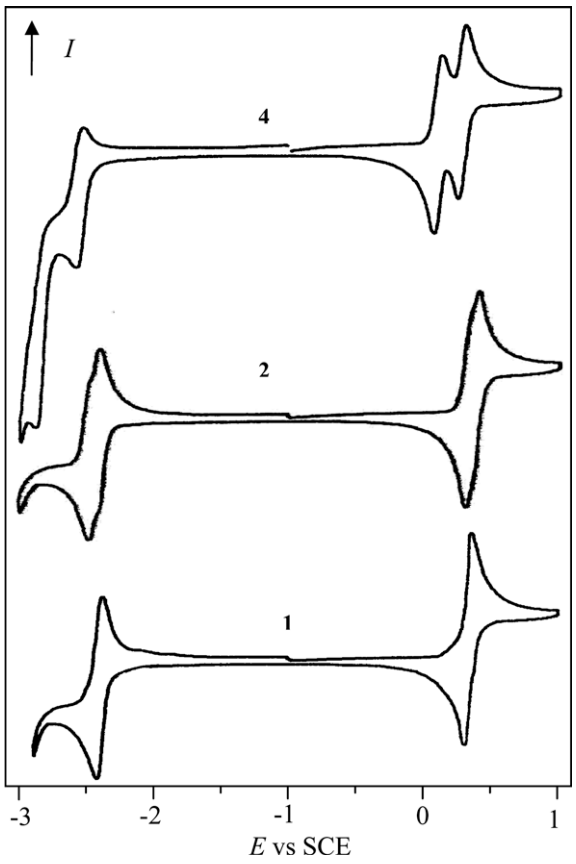

Fig. 6. Cyclic voltammograms of **1**, **2** and **4**.

Table 3
Formal electrode potentials (E_0 in V, versus SCE) and peak-to-peak separations (ΔE_p in mV) for **1**, **2** and **4**.

	1	2	4
$E_{1/2}(2-\|-)$/ V		−2.412	−2.862[b]
$E_{1/2}(-\|0)$/ V	−2.379	−2.336	−2.517
$\Delta E(2-\|-\|0)$/ mV		76	
K_c[a]		4.4×10^1	
$E_{1/2}(0\|+)$/ V	0.298	0.303	0.064
$E_{1/2}(+\|2+)$/ V		0.365	0.242
$\Delta E(0\|+\|2+)$/ mV		62	178
K_c[a]		2.2×10^1	7.06×10^3

[a] $\ln K_c = \Delta E \cdot F/RT$.
[b] E_{pc} of an irreversible wave.

to the Fe^{II}–Fe^{I} and Fe^{I}–Fe^{I} mono- and dianions, while the second reduction process is irreversible in case of **4**. Mixed-valence compounds have been intensely studied since they can be regarded as simple systems for testing electron-transfer models. Complexes featuring linked ferrocenium/ferrocene redox centres represent one of the most widely investigated families of mixed-valence systems [29]; however, examples of bridged ferrocenes bearing indenyl ligands are still relatively rare. The conproportionation constant $K_c = 7.06 \times 10^3$ of the mixed-valence species $\mathbf{4}^+$, indicates that this compound lies well inside the range of the slightly delocalised, weakly-interacting class II mixed-valence species within the Robin-Day classification [30].

The generally small peak-to-peak separation between individual oxidations (ΔE) is consistent with limited interaction between the metal centers and decreases in the order **4** > **2**, thereby reflecting the influence of the CMe_2 spacer in the latter complex. The effect of this alkyl spacer on ΔE is however obscured by the influence of permethylation of the ancillary ring in **4**, which had been demonstrated to have a decreasing effect on ΔE in related biferrocene systems [31]. The increase in ΔE for successive oxidations from 178 to 240 mV in the transition from **4** to the related biferrocene $[(\eta^5\text{-}C_5Me_5)Fe(\eta^5\text{-}C_5H_4)]_2$ [31] may demonstrate the effect of charge delocalization into the annelated arene ring in the former complex, which will result in a decrease of interaction between the metal centers. The observation that ΔE is more pronounced in the reduction waves than in the oxidation waves of **2** may be ascribed to the fact that different molecular orbitals are involved (LUMO and HOMO are represented by b_1^* and b_2 orbitals, respectively, in indenyl metal complexes [24]). The former, which represents the active orbital in reduction processes, involves more ligand character than the latter, thereby facilitating a superexchange mechanism.

The CV traces of the slipped Fe–Co-triple-decker complexes **3** and **5** showed no reversible features at all and will therefore not be discussed further. However, it is noteworthy to mention that in a recent study on indenyl-bridged diruthenium complexes a similar loss of electrochemical reversibility in respect to mononuclear precursor complexes had been observed [16].

3. Conclusion

The two binuclear complexes **2** and **4** bear non-coordinated ring systems, which act as diene ligands in the reaction with the triple-decker complex $[\{(\eta^5\text{-}Me_5C_5)Co\}_2(\mu\text{-}\eta^6\text{:}\eta^6\text{-toluene})]$ and substitute the toluene molecule under formation of the tetranuclear complex **3** and the trinuclear complex **5**, respectively, among other non-isolated products. Therefore, reactions of arene–metal complexes with non-coordinated ring systems provide a facile way to synthesize metallocenes of higher nuclearity and mixed metal complexes.

The $[(\eta^5\text{-}Me_5C_5)Co]$ fragment is interacting solely with the diene system of the non-junction carbon atoms of the six-membered indenyl rings of **2** and **4** in a η^4-fashion, while the junction carbon atoms are coordinated exclusively to $[(\eta^5\text{-}C_5R_5)Fe]$ fragments, thereby resulting in an overall $\mu\text{-}\eta^5\text{:}\eta^4$ coordination mode of the indenyl bridge. The coordination of the $[(\eta^5\text{-}Me_5C_5)Co]$ fragment results in a significant folding of the annelated arene ring along the vector C4–C7 and an elongation of the C–C bonds which link the η^5-cyclopentadienyl and the η^4-diene parts of the $\mu\text{-}\eta^5\text{:}\eta^4$-indenyl bridge.

While both the isolated $[(\eta^5\text{-}C_5R_5)_2Fe]$ system as well as the $[(\eta^5\text{-}C_5R_5)Co(\eta^4\text{-diene})]$ system show electrochemically reversible oxidation processes, will the fusion of these systems by means of a bridging $\mu\text{-}\eta^5\text{:}\eta^4$-indenyl ligand lead to the loss of reversibility in any electron-transfer step.

4. Experimental

4.1. General information

All manipulations were carried out under argon using Schlenk type glassware and techniques. All solvents were dried appropriately and distilled under argon prior to use. 2,2-Bis(1-indenyl)propane [32], 1,1′-biindene [33] $[\{(\eta^5\text{-}Me_5C_5)Co\}_2(\mu\text{-}\eta^6\text{:}\eta^6\text{-toluene})]$ [18], and $[(\eta^5\text{-}Me_5C_5)Fe(tmeda)Cl]$ [34] were prepared by published procedures.

4.2. X-ray data collection and structure solution and refinement

Crystals were selected under the microscope in a dry box, mounted in glass capillaries and measured on a STOE IPDSII diffractometer. Details of the data collections, structure solution and

refinement are given in Table 4. Several heavy atoms were readily located by direct methods (SHELXS-97 [35]). Difference Fourier analysis and least square cycles (SHELXL-97 [36]) allowed the location of the other atoms. The positions of hydrogen atoms were geometrically determined for all carbon atoms using the riding model with fixed bond lengths and fixed temperature factors for the refinement.

4.3. NMR-Spectroscopy

The NMR spectra were recorded at 300 K on a Bruker Avance 500 (^{1}H NMR 500 MHz, ^{13}C NMR 125 MHz) or on a Bruker AC300 (^{1}H NMR 300 MHz, ^{13}C NMR 75 MHz) spectrometer. ^{1}H NMR spectra were referenced to residual protons of the solvent, ^{13}C NMR to the solvent signal (C_6D_6: δ_H = 7.27 ppm, δ_C = 128.00 ppm) as standard. The numbering scheme of the indenyl signals is referred to Scheme 3 for reasons of comparability.

4.4. Cyclic voltammetry

Cyclic voltammetry experiments were performed in dimethoxyethane solution at −40 °C with a scan speed v of 100 mV s^{-1} in a three electrode array cell comprised of a glassy carbon working electrode, a platinum wire counter electrode and a reference saturated calomel electrode (SCE), separated from the solution via a salt bridge. The supporting electrolyte was 0.1 M (n-Bu)$_4$NClO$_4$. All potentials are referred to the saturated calomel electrode (SCE). In the case of nearly overlapping processes their separation has been evaluated by the Richardson-Taube method [37].

5. Synthesis

5.1. Complex **1**

4.75 mL of n-BuLi (2.5 M in hexane, 11.9 mmol) was slowly added to a solution of 2,2-bis(indenyl)propane (3 g, 11.0 mmol) in THF under stirring at −78 °C. The orange reaction mixture was slowly warmed to room temperature and C_5H_5Na (1 g, 11.0 mmol) in THF was added. The resulting mixture was added under stirring to a suspension of $FeCl_2$ (1.4 g, 11.0 mmol) in THF at −78 °C. The resulting suspension was stirred for 1 h at −78 °C and subsequently warmed to ambient temperature. The solvent was removed under vacuum, and the residue was extracted into ether. The resulting solution was filtered and concentrated in vacuo. Traces of by-products were removed by chromatography on alumina {0% H_2O, eluent: hexane/ether (4:1)}. Storage of the concentrated eluate at −30 °C for one week afforded red crystals of the title compound. Yield: 0.85 g (21%). Anal. Found: C, 79.60; H, 6.21%. $C_{26}H_{24}Fe$. Calc.: C, 79.59; H, 6.12. ^{1}H NMR (C_6D_6, 500 MHz, 300 K), δ (ppm): 1.94 (s, 3H, CH_3), 2.51 (s, 3H, CH_3), (d, 2H, H3′), 3.84 (t, 5H, C_5H_5), 4.18 (d, 1H, H2), 4,85 (m, 2H, H3), 5.96 (d, 1H, H2′), 6.81 (m, 2H, H5′, H6′), 7.09 (m, 2H, H5, H6), 7.27 (d, 1H, H7′), 7.48 (d, 1H, H4′), 7.38 (m, 1H, H7), 7.68 (m, 1H, H4). ^{13}C NMR (C_6D_6, 75 MHz, 297 K), δ (ppm): 26.86 (CH_3), 29.83 (CH_3), 35.7 (C3′′), 36.0 ($C(CH_3)_2$), 58.5 (C2), 67.92 (C_5H_5), 69.7 (C3), 85.4 (C1), 87.1 (C3a), 90.5 (C7a), 121.0 (C2′), 121.7, 122.3, 122.7, 124.4, 125.8, 126.8, 128.3, 128.4 (C4–C7, C4′–C7′), 142.7, 144.3 (C3a′, C7a′), 151.4 (C1′). m/z (EI) 392 (100%, M$^+$), 377 (91), 277 (52), 121 (33), 115 (20).

5.2. Complex **2**

The procedure described above afforded the dinuclear complex **2** as a mixture of isomers under the respective use of 2,2-bis(1-indenyl)propane (3 g, 11.0 mmol), 9.5 ml of n-BuLi (2.5 M in hexane, 23.8 mmol), C_5H_5Na (2 g, 22.0 mmol), and $FeCl_2$ (2.79 g, 22.0 mmol). The product mixture was subjected to column chromatography on alumina {0% H_2O, eluent: hexane/ether (4:1)}.The red eluate containing the product was concentrated and stored at −30 °C. After one week the title compound was obtained as red crystals in a yield of 1.014 g (18%). Anal. Found: C, 72.46; H, 5.56%. $C_{31}H_{28}Fe_2$. Calc.: C, 72.65; H, 5.46. ^{1}H NMR (C_6D_6, 500 MHz, 300 K), δ (ppm): 2.55 (s, 6H, CH_3), 3.83 (s, 10H, C_5H_5), 4.01 (d, 2H, H2), 4.75 (d, 2H, H3), 6.80 (m, 4H, H5, H6), 7.40 (m, 2H, H7), 7.73 (m, 2H, H4). ^{13}C NMR (C_6D_6, 75 MHz, 297 K), δ (ppm): 32.43 ($C(CH_3)_2$), 36.28 ($C(CH_3)_2$), 60.05 (C2), 69.32 (C_5H_5), 70.41 (C3), 85.39 (C1), 88.53 (C7a), 93.48 (C3a), 122.87, 122.88 (C5, C6), 128.47 (C7), 128.53 (C4). m/z (EI) 512 (100%, M$^+$), 497 (36), 447 (60), 326 (42), 277 (21), 121 (15).

5.3. Complex **3**

A solution of [{(η^5-Me_5C_5)Co}$_2$(μ-η^6:η^6-toluene)] (0.14 g, 0.29 mmol) in ether was slowly added to a solution of **2** (0.15 g, 0.29 mmol, mixture of isomers as received from the previous reaction) in ether which was cooled to −78 °C. During the addition the colour changed from red to brown. After stirring the reaction mixture for 1 h at −78 °C it was slowly warmed to room temperature. The reaction mixture was concentrated, filtered and stored at −30 °C. After one week the product was obtained as brown crystals in a yield of 37 mg (14%). ^{1}H NMR (C_6D_6, 500 MHz, 300 K), δ (ppm): 1.33 (s, 30H, $C_5(CH_3)_5$), 1.76 (s, 6H, $C(CH_3)_2$), 1.97 (m, 2H, H4), 2.41 (m, 2H, H7), 3.89 (s, 10H, C_5H_5), 3.99 (d, 2H, H2), 4.83 (d, 2H, H3), 5.76 (m, 2H, H5), 5.92 (m, 2H, H6). ^{13}C NMR (C_6D_6, 75 MHz, 297 K), δ (ppm): 9.63 ($C_5(CH_3)_5$)), 31.49 ($C(CH_3)_2$), 34.83 ($C(CH_3)_2$), 51.59, 52.73 (C4, C7), 59.79 (C2), 62.72 (C3), 70.82 (C_5H_5), 81.54, 81.85 (C5, C6), 88.49 ($C_5(CH_3)_5$), 91.18, 92.46, 92.93 (C1, C3a, C7a). m/z (EI) 892 (4%, M$^+$), 771 (21), 706 (49), 585 (100), 512 (23), 277 (16).

5.4. meso-**4**

A solution of dilithium 1,1′-biindenyl (1.94 g, 8.0 mmol) in THF was added dropwise under stirring to a suspension of [(η^5-Me_5C_5)Fe(tmeda)Cl] (5.49 g, 16.0 mmol) in THF at −78 °C. The reaction mixture was slowly warmed to room temperature and the colour changed to ruby red. The solvent was removed in vacuo, and the residue was extracted into pentane, concentrated, and crystallized at –30 °C. Yield: 2.6 g (53%). ^{1}H NMR (C_6D_6, 500 MHz, 300 K), δ (ppm): 7.47 (m, 2H, H4), 7.07 (m, 2H, H7), 6.71 (m, 4H, H5, H6), 4.26 (d, 2H, H2), 4.17 (d, 2H, H3), 1.06(s, 30H, $C_5(CH_3)_5$). ^{13}C NMR (C_6D_6, 75 MHz, 297 K), δ (ppm): 129.4, 128.5 (C4, C7), 122.4, 122.2 (C5, C6), 89.6, 86.1 (C3a, C7a), 77.8 ($C_5(CH_3)_5$), 76.8 (C1), 74.3, 66.8 (C2, C3), 9.7 ($C_5(CH_3)_5$). m/z (ESI, CH_3OH) 610 (100%, M$^+$).

5.5. Complex **5**

An ethereal solution of *meso*-**4** (0.42 g, 0.7 mmol) was added to a solution of [{(η^5-Me_5C_5)Co}$_2$(μ-η^6:η^6-toluene)] (0.34 g, 0.7 mmol) in ether at −78 °C under stirring. The reaction mixture was stirred for 2 h at −78 °C and then slowly warmed to room temperature and stirred for further 2 days. The colour of the solution changed from dark brown to reddish-brown. The reaction mixture was concentrated, filtered and stored at −30 °C. After one week the product was obtained as brown crystals. Yield, 0.31 g (51.4%). ^{1}H NMR (C_6D_6, 500 MHz, 300 K), δ (ppm): 7.94, 7.36 (2 d, 2 × 1H, H7′, H4′), 7.08 (t, 2H, H5′, H6′), 6.10, 6.13 (2 d, 2 × 1H, H5, H6), 4.39, 4.27 (2 s, 2 × 1H, H3, H3′), 4.02, 3.47 (2 s, 2 × 1H, H2, H2′), 2.49, 2.19 (2 s, 2 × 1H, H4, H7), 1.85, 1.81 (2 s, 2 × 15H, $FeC_5(CH_3)_5$), 1.66 (s, 15H, $CoC_5(CH_3)_5$). ^{13}C NMR (C_6D_6, 75 MHz,

Table 4
Crystallographic data of **1**, *meso*-**2**, *rac*-**3**, *meso*-**4** and **5**.[a]

	1	*meso*-**2**	*rac*-**3**	*meso*-**4**	**5**
Empirical formula	$C_{26}H_{24}Fe$	$C_{31}H_{28}Fe_2$	$C_{51}H_{58}Co_2Fe_2$	$C_{19}H_{22}Fe$	$C_{52}H_{67}CoFe_2O$
Formula weight	392.30	512.23	900.53	306.22	878.69
Measurement temperature	150(2)	150(2)	150(2)	150(2)	150(2)
Wavelength (Å)	0.71073	0.71073	0.71073	0.71073	0.71073
Crystal system	Monoclinic	Monoclinic	Triclinic	Monoclinic	Orthorhombic
Space group	$P2_1$	$P2_1/n$	$P\bar{1}$	$P2_1/n$	$P2_12_12_1$
Unit cell dimensions					
a (Å)	8.6345(17)	8.6540(17)	11.983(2)	13.327(3)	8.5301(17)
b (Å)	10.496(2)	19.784(4)	12.799(3)	8.4156(17)	13.382(3)
c (Å)	10.647(2)	13.666(3)	15.006(3)	13.878(3)	39.568(8)
α (°)	90.50(3)	101.89(3)	78.19(3)	100.81(3)	
β (°)			78.45(3)		
γ (°)			67.22(3)		
Volume (Å^3)	964.9(3)	2289.6(8)	2058.5(7)	1528.8(5)	4516.5(16)
Z	2	4	2	4	4
D_{calc} (Mg/m^3)	1.350	1.486	1.453	1.330	1.292
Absorption coefficient (mm^{-1})	0.789	1.285	1.518	0.974	1.033
$F(000)$	412	1064	940	648	1864
Crystal size (mm^3)	0.16 × 0.14 × 0.12	0.23 × 0.14 × 0.13	0.28 × 0.17 × 0.16	0.36 × 0.34 × 0.15	0.28 × 0.26 × 0.25
Crystal colour	Red	Red	Brown	Brown	Brown
2θ Range (°)	1.91–25.00	1.84–27.07	1.74–27.30	1.94–27.14	1.61−27.27
Index range	$-10 \leqslant h \leqslant 10$	$-11 \leqslant h \leqslant 11$	$-15 \leqslant h \leqslant 15$	$-17 \leqslant h \leqslant 16$	$-10 \leqslant h \leqslant 10$
	$-12 \leqslant k \leqslant 12$	$-23 \leqslant k \leqslant 25$	$-16 \leqslant k \leqslant 16$	$-10 \leqslant k \leqslant 10$	$-17 \leqslant k \leqslant 17$
	$-12 \leqslant l \leqslant 12$	$-17 \leqslant l \leqslant 17$	$-19 \leqslant l \leqslant 19$	$-17 \leqslant l \leqslant 17$	$-50 \leqslant l \leqslant 50$
Collected reflections	12301	15484	31884	23132	55647
Independent reflections (R_{int})	3399 (0.2020)	4953 (0.1398)	9004 (0.1175)	3360 (0.1005)	9858 (0.1075)
Refinement method	Full-matrix least-squares on F^2	Full-matrix least-squares on F^2	Full-matrix least-squares on F^2	Full-matrix least-squares on F^2	Full-matrix least-squares on F^2
Parameters	244	298	496	181	505
Goodness-of-fit on F^2	1.051	1.143	1.160	1.018	0.890
Data [$I > 2\sigma(I)$]	2220	3221	5986	2583	6840
Final R indices [$I > 2\sigma(I)$]	$R_1 = 0.0895$	$R_1 = 0.0855$	$R_1 = 0.0842$	$R_1 = 0.0418$	$R_1 = 0.0467$
	$wR_2 = 0.1261$	$wR_2 = 0.1517$	$wR_2 = 0.1341$	$wR_2 = 0.0861$	$wR_2 = 0.0995$
R Indices for all data	$R_1 = 0.1451$	$R_1 = 0.1410$	$R_1 = 0.1379$	$R_1 = 0.0651$	$R_1 = 0.0722$
	$wR_2 = 0.1442$	$wR_2 = 0.1688$	$wR_2 = 0.1509$	$wR_2 = 0.0938$	$wR_2 = 0.1059$

[a] See Supplementary Section.

297 K), δ (ppm): 131.5, 129.7 (C4′, C7′), 122.8, 120.9 (C5′, C6′), 96.3, 94.8 (C3a, C7a), 89.4 (C3a′), 89.0 ($Fe'C_5(CH_3)_5$), 84.0 (C7a′), 83.9, 82.3 (C5, C6), 80.6 (C1), 80.5 ($CoC_5(CH_3)_5$), 77.9 ($FeC_5(CH_3)_5$), 77.8 (C1′), 75.1 (C3′), 68.4, 66.7, 65.8 (C3, C2, C2′), 51.9, 50.5 (C4, C7). 11.2, 11.1, 10.9 (CH_3 of Cp^*Fe, Cp^*Fe', Cp^*Co).

Supplementary material

CCDC 711914, 711915, 711916, 711917, 711918 contain the supplementary crystallographic data for **1**, **2**, **3**, **4**, **5**. These data can be obtained free of charge from The Cambridge Crystallographic Data Centre via www.ccdc.cam.ac.uk/data_request/cif.

Acknowledgments

This work was supported by the DFG. We thank Prof. B. Albert for making measuring time possible at the X-ray facility of the Eduard-Zintl Institute. We thank Dr. Bernd Bachmann, for a gift of 2,2-bis(1-indenyl)propane.

References

[1] J.M. O'Connor, C.P. Casey, Chem. Rev. 87 (1987) 307.
[2] T.B. Marder, D.C. Roe, D. Milstein, Organometallics 7 (1988) 1451.
[3] P. Caddy, M. Green, L.E. Smart, N. White, J. Chem. Soc., Chem. Commun. (1978) 839.
[4] A. Borrini, P. Diversi, G. Ingrosso, A. Lucherini, G. Serra, J. Mol. Catal. 30 (1985) 181.
[5] (a) H. Bönnemann, Angew. Chem. 97 (1985) 264;
(b) H. Bönnemann, Angew. Chem., Int. Ed. Engl. 24 (1985) 248.
[6] A. Ceccon, S. Santi, L. Orian, A. Bisello, Coord. Chem. Rev. 248 (2004) 683.
[7] V. Cadierno, J. Díez, M.P. Gamasa, J. Gimeno, E. Lastra, Coord. Chem. Rev. 193–195 (1999) 147.
[8] Stradiotto, McGlinchey, Coord. Chem. Rev. 219–221 (2001) 311.
[9] M.L.H. Green, N.D. Lowe, D. O'Hare, J. Chem. Soc., Chem. Commun. (1986) 1547.
[10] A. Ceccon, A. Gambaro, S. Santi, G. Valle, A. Venzo, J. Chem. Soc., Chem. Commun. (1989) 51.
[11] C. Bonifaci, A. Ceccon, A. Gambaro, P. Ganis, S. Santi, G. Valle, A. Venzo, Organometallics 12 (1993) 4211.
[12] C. Bonifaci, A. Ceccon, A. Gambaro, P. Ganis, S. Santi, G. Valle, A. Venzo, J. Organomet. Chem. 492 (1995) 35.
[13] C. Bonifaci, G. Carta, A. Ceccon, A. Gambaro, S. Santi, A. Venzo, Organometallics 15 (1996) 1630.
[14] P. Ceccetto, A. Ceccon, A. Gambaro, S. Santi, P. Ganis, R. Gobetto, G. Valle, A. Venzo, Organometallics 17 (1998) 752.
[15] A.R. Kudinov, P.V. Petrovskii, Yu.T. Struchkov, A.I. Yanovskii, M.I. Rybinskaya, J. Organomet. Chem. 421 (1991) 91.
[16] E.V. Mutseneck, Z.A. Starikova, K.A. Lyssenko, P.V. Petrovskii, P. Zanello, M. Corsini, A.R. Kudinov, Eur. J. Inorg. Chem. (2006) 4519.
[17] J.M. Manriquez, L. Valle, E.E. Bunel, Organometallics 4 (1985) 1680.
[18] J.J. Schneider, U. Denninger, O. Heinemann, C. Krüger, Angew. Chem. 107 (1995) 631; J.J. Schneider, U. Denninger, O. Heinemann, C. Krüger, Angew. Chem., Int. Ed. Engl. 34 (1995) 592.
[19] J.J. Schneider, Z. Naturforsch. 50b (1995) 1055.
[20] S. Guo, R. Hauptmann, J.J. Schneider, Z. Anorg. Allg. Chem. 633 (2007) 2332.
[21] P.G. Jones, H. Hopf, T. Hartig, Acta Crystallogr. E 58 (2002) m139.
[22] D. Tews, P.E. Gaede, Organometallics 23 (2004) 968.
[23] O.J. Curnow, G.M. Fern, J. Organomet. Chem. 690 (2005) 3018.
[24] M.J. Calhorda, L.F. Veiros, J. Organomet. Chem. 635 (2001) 197.
[25] S.A. Westcott, K. Kakkar, G. Stringer, N.J. Taylor, T.B. Marder, J. Organomet. Chem. 394 (1990) 777.
[26] T.S. Piper, G. Wilkinson, J. Inorg. Nucl. Chem. 3 (1956) 104.
[27] F.H. Köhler, G. Matsubayashi, J. Organomet. Chem. 96 (1975) 391.
[28] R.B. Materikova, V.N. Babin, I.R. Lyatifov, T.K. Kurbanov, E.I. Fedin, P.V. Petrovskii, A.I. Lutsenko, J. Organomet. Chem. 142 (1977) 81.
[29] S. Barlow, D. O'Hare, Chem. Rev. 97 (1997) 637.
[30] M.B. Robin, P. Day, Adv. Inorg. Chem. Radiochem. 10 (1967) 247.
[31] M.-H. Delville, S. Rittinger, D. Astruc, J. Chem. Soc., Chem. Commun. (1992) 519.
[32] I.E. Nifantév, P.V. Ivchenko, L.G. Kuz'mina, Y.N. Luzikov, A.A. Sitnikov, O.E. Sizan, Synthesis (1997) 469.
[33] N.E. Heimer, M. Hojjatie, C.A. Panetta, J. Org. Chem. 47 (1982) 2593.
[34] K. Jonas, P. Klusmann, R. Goddard, Z. Naturforsch. 50 B (1995) 394.
[35] G.M. Sheldrick, SHELXS-97, Program for the Solution of Crystal Structures, Universität Göttingen, 1997.
[36] G.M. Sheldrick, SHELXL-97, Program for the Refinement of Crystal Structures, Universität Göttingen, 1997.
[37] D.E. Richardson, H. Taube, Inorg. Chem. 20 (1981) 1278.